Title Page

Copper increases reductive dehalogenation of haloacetamides by zero-valent iron in drinking water: reduction efficiency and integrated toxicity risk

Wenhai Chu[a,*], Xin Li[a], Tom Bond[b], Naiyun Gao[a], Xu Bin[a], Qiongfang Wang[a], Sunke Ding[a]

[a]*State Key Laboratory of Pollution Control and Resources Reuse, College of Environmental Science and Engineering, Tongji University, Shanghai, 200092, China*

[b] *Department of Civil and Environmental Engineering, Imperial College London, London SW7 2AZ, UK*

* Corresponding author.

Address: College of Environmental Science and Engineering, Tongji University, Room 308 Mingjing Building, 1239 Siping Road, Yangpu District, Shanghai, 200092, China

Tel: +86 021 65982691; Fax: +86 021 65986313;

E-mail address: feedwater@126.com; 1world1water@tongji.edu.cn

ABSTRACT

The haloacetamides (HAcAms), an emerging class of nitrogen-containing disinfection byproducts (N-DBPs), are highly cytotoxic and genotoxic, and typically occur in treated drinking waters at low μg/L concentrations. Since many drinking distribution and storage systems contain unlined cast iron and copper pipes, reactions of HAcAms with zero-valent iron (ZVI) and metallic copper (Cu) may play a role in determining their fate. Moreover, ZVI and/or Cu are potentially effective HAcAm treatment technologies in drinking water supply and storage systems. This study reports that ZVI alone reduces trichloroacetamide (TCAcAm) to sequentially form dichloroacetamide (DCAcAm) and then monochloroacetamide (MCAcAm), whereas Cu alone does not impact HAcAm concentrations. The addition of Cu to ZVI significantly improved the removal of HAcAms, relative to ZVI alone. TCAcAm and their reduction products (DCAcAm and MCAcAm) were all decreased to below detection limits at a molar ratio of ZVI/Cu of 1:1 after 24 h reaction (ZVI/TCAcAm = 0.18 M/5.30 μM). TCAcAm reduction increased with the decreasing pH from 8.0 to 5.0, but values from an integrated toxic risk assessment were minimised at pH 7.0, due to limited removal MCAcAm under weak acid conditions (pH = 5.0 and 6.0). Higher temperatures (40 ^{o}C) promoted the reductive dehalogenation of HAcAms. Bromine was preferentially removed over chlorine, thus brominated HAcAms were more easily reduced than chlorinated HAcAms by ZVI/Cu. Although tribromoacetamide was more easily reduced than TCAcAm during ZVI/Cu reduction, treatment of tribromoacetamide resulted in a higher integrated toxicity risk than TCAcAm, due to the formation of monobromoacetamide (MBAcAm).

Keywords:

Disinfection byproducts; Haloacetamides; Dechlorination; Zero-valent iron/Copper; Integrated toxicity risk; Drinking water

1. Introduction

Nitrogenous disinfection by-products (N-DBPs) have received increasing attention because they are more toxic than the regulated trihalomethanes (THMs) and haloacetic acids (HAAs) (Plewa et al., 2007, 2008; Yang and Zhang, 2013; Liu and Zhang, et al., 2014; Chu et al., 2015a). As a result of rapid population growth and rising water demand, drinking water source waters are facing threats of insufficiently treated wastewater discharges and algal blooms (Shah and Mitch, 2012; Chu et al., 2015b). These polluted water sources are characterized by higher levels of dissolved organic nitrogen (Dotson and Westerhoff, 2009; Liu et al., 2013), , which is linked to their frequent occurrence in chlor(am)inated drinking water (Krasner et al., 2006, 2013; Richardson et al., 2008, 2014; Goslan, et al., 2009; Bond et al., 2011, 2015; Chu et al., 2012; Hou et al., 2012). Among these N-DBPs, haloacetamides (HAcAms) were found to be highly cytotoxic and genotoxic in mammalian cell assays, i.e. 142 × more cytotoxic and 12 × more genotoxic than HAAs (Plewa et al., 2007; Richardson et al., 2007). They are the most cytotoxic of all DBP classes measured to-date, and are the second-most genotoxic DBP class, just behind the halonitriles (Plewa and Wagner, 2015; Richardson and Postigo, 2015). Among HAcAms, dichloroacetamide (DCAcAm) is typically found at the highest concentration, with trichloroacetamide (TCAcAm) and monochloroacetamide (MCAcAm) reported infrequently in low-bromide sources (Krasner et al., 2006; Richardson et al., 2007; Chu et al., 2012). The elevated toxicity of TCAcAm and DCAcAm were also observed in the recent studies based on metabonomics (Zhang et al., 2013; Yu et al., 2015), and DCAcAm presented significantly higher cytotoxicity and genotoxicity than halomethanes (Yang et al., 2014). While chlorinated HAcAms tend to occur at higher concentrations than their brominated analogues in drinking water (Krasner et al., 2006; Bond et al., 2011; Chu et al., 2012), the latter are actually more

cytotoxic and genotoxic (Plewa et al., 2008), Therefore, it is important to control both chlorinated and brominated HAcAms in drinking water.

Generally, DBP control strategies can be divided into three categories: (1) removal of DBP precursors prior to disinfection, (2) modification of disinfection practices to minimize DBP formation, and (3) removal of DBPs after formation. It has been reported that various pre-treatments in drinking water treatment plants (DWTPs) can achieve good removal of HAcAm precursors (Chu et al., 2011, 2014, 2015a; Xie et al., 2013), as well as for other N-DBPs (Bond et al., 2011; Shah et al., 2012). Efforts have also been made to study HAcAm formation mechanisms with the purpose of acquiring the knowledge to reduce their formation during chlorination (Shah and Mitch et al, 2012; Huang et al., 2012; Wang et al., 2014; Chu et al., 2015b). However, DBP formation can also occur in water distribution systems, due to reactions involving residual chlorine (Rossman et al., 2001). There remains an information gap on the removal of N-DBPs after their formation.

The polar nature of HAcAms (Figure SM1), including MCAcAm, DCAcAm and TCAcAm, suggests that reductive dehalogenation is a potential route for their removal. Furthermore, the end products of dehalogenation (i.e. non-chlorinated acetamide) are of low-toxicity to humans and the environment (Plewa et al., 2008). This motivated us to consider the potential of reductive dehalogenation technologies to reduce the levels of HAcAms in drinking water.

Since Gillham and O'Hannesin discovered that metallic iron fillings could be utilized in groundwater remediation (Gillham and O'Hannesin, 1994), the use of zero-valent iron (ZVI, Fe^0) for in-situ remediation of groundwater contaminated by chlorinated organic compounds has received considerable attention (Dries et al., 2004; He et al., 2010; Kohn et al., 2005; Liu and Lowry, 2006; Zhang et al., 2011). Moreover, to enhance dehalogenation and prolong the activity of ZVI, a

second transition metal (e.g. Pd, Ni, Ru and Pt) with high hydrogenation ability can be incorporated in a bimetal system, such as applied for the remediation of carbon tetrachloride (Feng and Lim, 2007; Wang et al., 2009), chloroform (Feng and Lim, 2007; Wang et al., 2009), dichloromethane (Feng and Lim, 2007; Wang et al., 2009), tetrachloroethylene (Lien and Zhang, 2001; Zhang et al., 1998), trichloroethylene (Lien and Zhang, 2001; Tee et al., 2009; Zhang et al., 1998), dichloroethene (Lien and Zhang, 2001; Zhang et al., 1998), 1,1-dichloroethane (Cwiertny et al., 2006), 1,1,1-trichloroethane (Cwiertny et al., 2006; Lien and Zhang, 2001, and 1,1,2,2-tetrachloroethane (Lien and Zhang, 2005)

Finished drinking water is often distributed from DWTPs to consumers by unlined cast iron pipes, and sometimes copper pipes (Ridgway et al, 1981; McNeill et al, 2001; Lin et al, 2001; Niquette et al, 2000). During distribution, drinking water is also often stored in storage ponds made from iron materials, with copper materials also sometimes used to inhibit the growth of microorganisms (Kooij et al, 2005; Teng et al, 2008; Critchley et al, 2001; Lehtola et al, 2004). It is important to proactively examine the potential of ZVI, Cu, and their combination (ZVI/Cu) for the reductive dehalogenation of HAcAms and possible application in drinking water distribution and storage systems. Therefore, the objective of this study was to examine the potential of three reductive dehalogenation technologies - ZVI alone, Cu alone, and combined ZVI/Cu - for removing HAcAms in drinking water. This is the first study to report findings about N-DBP removal by reductive dehalogenation methods. Both chlorinated and brominated HAcAms were considered. The changes of HAcAms concentrations and integrated toxic risk caused by HAcAms were also examined.

2. Materials and methods

2.1. Materials

MCAcAm (98.5%), DCAcAm (98.5%) and TCAcAm (99%) standards were obtained from Alfa Aesar (Karlsruhe, Germany), and five bromine-containing HAcAms (bromochloroacetamide [BCAcAm], dibromoacetamide [DBAcAm], bromodichloroacetamide [BDCAcAm], dibromochloroacetamide [DBCAcAm] and tribromoacetamide [TBAcAm]) were purchased from Orchid Cellmark (New Westminster, BC, Canada). Monobromoacetamide (MBAcAm) and three HAAs (monochloroacetic acid [MCAA], dichloroacetic acid [DCAA] and trichloroacetic acid [TCAA]) were supplied by Sigma-Aldrich (St Louis, Missouri, USA). Sodium acetate anhydrous, 2-(N-morpholino)ethanesulfonic acid (MES, 99%) and tris(hydroxymethy)aminomethane (TRIS, 99.9%) were purchased from Aladdin Industrial Inc (Shanghai, China). The ZVI (≥99.99%) and copper (≥99.99%) powders were also supplied by Sigma-Aldrich (St Louis, Missouri, USA). Ultrapure water was produced with a Millipore Milli-Q Gradient water purification system (Billerica, MA, USA). All the other chemical reagents were at least of analytical grade, and obtained from Sinopharm Chemical Reagent Co., Ltd (Shanghai, China) unless otherwise noted.

2.2. Experimental procedure

Batch reduction tests were performed by adding selected doses of ZVI and/or Cu powder (doses range: ZVI = 0.2~10.0 g/L [0.004~0.179 M]; ZVI/Cu molar ratio = 1:1, except as noted) to 250-mL sealed glass bottles containing 50 mL one of the following trihalogenated HAcAms: TCAcAm, BDCAcAm, DBCAcAm or TBAcAm (5.30 μM, except as noted). Before each experiment the reaction bottles were purged with nitrogen to remove air. Each run lasted for 24 h and the bottles were placed on a water bath shaker at 150 r/m to make the solid and liquid well-mixed and keep the

125 temperature constant at 25 ±0.2 °C unless otherwise noted. Sodium acetate (0.1 M), MES (0.03 M)
126 and Tris (0.05 M) were used as a pH 7.0 ±0.2 buffer (Keenan and Sedlak, 2008) unless otherwise
127 noted.

128 **2.3. Analytical methods**

129 At selected time intervals, 10 mL of reaction solution was filtered through 0.22 μm syringe filters
130 and 4 g anhydrous sodium sulfate was added into the filtered sample. Then HAcAms were
131 immediately extracted into 2mL methyl tert-butyl ether (MTBE), and were analyzed using gas
132 chromatography (GC) coupled with an electron capture detector (ECD) (QP 2010 plus, Shimadzu,
133 Japan). Injections of 1.0 μL of the extract were introduced via a splitless injector onto a GC column
134 (RTX-5, 30-m × 0.25-mm ID, 0.25-μm film thickness). The column oven was initially held at 40 °C
135 for 10min, ramping to 200 °C at 20 °C/min and holding for 2 min. The injection port was controlled
136 at 180 °C and the ECD detector temperature was 320 °C. Three HAAs (MCAA, DCAA and TCAA)
137 were also analyzed by the GC/ECD (QP 2010 plus, Shimadzu, Japan) according to US EPA method
138 552.2 (USEPA, 1995; Chu et al, 2014). The detection limits for TCAcAm, DCAcAm, MCAcAm,
139 TCAA, DCAA, and MCAA were 0.01, 0.01, 0.05, 0.05, 0.05, and 0.07 μM, respectively.
140 Brominated HAcAms, were analyzed by combining high pressure liquid chromatography and triple-
141 quadrupole mass spectrometry (HPLC/tqMS). The HPLC (e2695) from Waters (Milford, MA),
142 employing a Hypersil GOLD C18 packed column (100 × 2.1 mm i.d., 5 μ m) with a Hypersil GOLD
143 precolumn (10 × 2.1 mm i.d., 5 μ m) (Thermo Scientific; Waltham, MA) was used for separation.
144 After separation, a tqMS (TSQ Quantum Access MAX) from Thermo Scientific (Waltham, MA)
145 was used to detect all brominated HAcAms by positive atmospheric pressure chemical ionization
146 combined with the selective reaction monitoring mode. The optimal operating parameters were as

147 follows: discharge current at 4.0 μA, vaporizer temperature at 350 ℃, sheath gas pressure at 40 psi,
148 capillary temperature at 250 ℃, and collision pressure at 1.5 m Torr. Detection limits for all
149 brominated HAcAm were below 0.01 μM. More details of the DBP analyses are presented
150 elsewhere (Krasner et al., 2006; Chu et al., 2012, 2014). All samples were prepared in triplicate and
151 the error bars in the figures represent the standard deviations from triplicate measurements. Relative
152 standard deviations (n = 3) of all samples were all below 7%.

153 ## 3. Results and discussion

154 ### 3.1. Reduction of chlorinated HAcAms by ZVI

155
156 **[Figure 1]**
157

158 Figure 1 shows the time-dependent changes of concentrations for three chlorinated HAcAms
159 (TCAcAm, DCAcAm and MCAcAm) at different ZVI doses. As shown in Figure 1a, at a low ZVI
160 dose (0.2 g/L), TCAcAm concentrations slightly decreased from the initial 5.30 ± 0.27 μM to 4.57
161 ± 0.23 μM over 24 h, which equates to a very low pseudo-first-order reduction rate of 0.01 h^{-1} (Table
162 SM1). In contrast, at higher ZVI doses (5.0 g/L and 10.0 g/L), TCAcAm concentrations presented
163 a significant reduction and the pseudo-first-order reduction rate increased to 0.18 h^{-1} and 0.43 h^{-1},
164 respectively (Table SM1). After 24 h, TCAcAm was completely removed at ZVI doses of 5.0 g/L
165 and 10.0 g/L.

166 As shown in Figure 1b and 1c, DCAcAm and MCAcAm were both undetectable after 24 h at
167 the lowest ZVI dose (0.2 g/L). This indicated the slight reduction of TCAcAm at the low ZVI dose
168 (0.2 g/L) was probably due to the very slow hydrolysis of TCAcAm at pH 7.0 (Glezer et al., 1999;
169 Reckhow et al., 2001; Chu et al., 2009a), as shown in Equation (1), rather than dechlorination. It

should be noted that the hydrolysis of TCAcAm, DCAcAm and MCAcAm is all negligible in 24 h when solution pH is lower than 7.0 (Chu et al., 2009a, 2013). This was also been confirmed by our control experiments. When the ZVI dose increased to 5.0 g/L, DCAcAm concentrations increased from initial value of < 0.01 μM to 1.64 ±0.08 μM and 1.67 ±0.08 μM after 6 h and 12 h respectively, before decreasing to 0.92 ±0.05 μM at 24 h (Figure 1b). Data at 10.0 g/L followed a similar pattern, except no DCAcAm was detected after 24 h. Furthermore, MCAcAm increased over a 24 h period, from an initial value below the detection limit to 0.47 μM (ZVI dose = 5.0 g L^{-1}). At a higher dose of ZVI (10 g L^{-1}), MCAcAm first increased to 0.58 ±0.03 μM after 12 h and then decreased to 0.26 ±0.01 μM by 24 h. (Figure 1c). As shown in Figure 1d, the sum of three HAcAm concentrations also decreased as the ZVI dose increased from 0.2 g/L to 10.0 g/L. The enhancement in the reduction of three HAcAms with increasing ZVI dosages was probably due to the increasing availability of adsorption/reduction sites at the higher doses (Wang and Zhang, 1997; Xia et al., 2014).

Many environmentally significant contaminants, such as the chlorinated hydrocarbons mentioned above, can serve as the ultimate electron acceptors during reductive dehalogenation. Likewise, the reduction of HAcAms by different iron species is essentially a surface-mediated, electrocatalytic reaction. Generally, the possible dehalogenation pathways for these contaminants can be divided into three categories: (i) direct electron transfer from ZVI to chlorinated hydrocarbons; (ii) reduction by ferrous iron (Fe^{2+}) formed from ZVI reduction; and (iii) electrocatalytic reduction by hydrogen formed from ZVI reduction (Guan et al., 2015). We examined the impact of Fe^{2+} by dosing Fe^{2+} instead of ZVI under the same reaction conditions, and found TCAcAm concentrations did not significantly change, and DCAcAm and MCAcAm were not detected over 24 h (Figure SM2). Most researchers accept that the reductive dechlorination of

chlorinated organics occurs on the surface of ZVI by pathway (i) (Equation 2-6), because the reduction rate of chlorinated organics by pathways (ii) and (iii) is very slow (House et al., 1972; Warren et al., 1995; Maithreepala et al., 2004). Based on dechlorination pathway (i) (direct electron transfer from iron to chlorinated hydrocarbons), the dechlorination of TCAcAm, DCAcAm and MCAcAm by ZVI can be represented as follows:

$$CCl_3CONH_2 + H_2O \rightarrow CCl_3COOH + NH_3 \quad (1)$$

(TCAcAm) (TCAA)

$$CCl_3CONH_2 + H^+ + Fe^0 \rightarrow CCl_2HCONH_2 + Fe^{2+} + Cl^- \quad (2)$$

(TCAcAm) (DCAcAm)

$$CCl_2HCONH_2 + H^+ + Fe^0 \rightarrow CClH_2CONH_2 + Fe^{2+} + Cl^- \quad (3)$$

(DCAcAm) (MCAcAm)

$$CClH_2CONH_2 + H^+ + Fe^0 \rightarrow CH_3CONH_2 + Fe^{2+} + Cl^- \quad (4)$$

(MCAcAm) (AcAm)

$$CCl_3CONH_2 + 2H^+ + 2Fe^0 \rightarrow CClH_2CONH_2 + 2Fe^{2+} + 2Cl^- \quad (5)$$

(TCAcAm) (MCAcAm)

$$CCl_3CONH_2 + 3H^+ + 3Fe^0 \rightarrow CH_3CONH_2 + 3Fe^{2+} + 3Cl^- \quad (6)$$

(TCAcAm) (AcAm)

$$[Fe^{2+}] = [DCAcAm] + 2[MCAcAm] + 3[AcAm] \quad (7)$$

As shown by Equation (2), reduction of 1 M TCAcAm to DCAcAm will produce 1 M Fe^{2+}. As

shown in Equation (5), generated by merging Equations (2) and (3), if 1 M TCAcAm is reduced to MAcAm, 2 M Fe^{2+} will be formed. Similarly, if 1 M TCAcAm was reduced to acetamide (AcAm), 3 M Fe^{2+} will be formed (Equation 6, generated by merging Equations (2), (3) and (4)). Therefore, the Fe^{2+} formed by dechlorination of TCAcAm with ZVI should theoretically equal the sum of [DCAcAm], twice the [MCAcAm] and three times [AcAm] (AcAm concentration is equal to the initial TCAcAm minus the remaining TCAcAm as well as the formation of DCAcAm and MCAcAm), with concentrations in moles (Equation 7). As shown in Figure 1e, there is a good correlation between the theoretical Fe^{2+} concentrations calculated using the equations above and the actual detected Fe^{2+} concentrations from 1 h to 24 h at pH 7.0. Further, the actual detected Fe^{2+} concentrations was slightly lower than the theoretical calculated Fe^{2+} (the slope is 1.19), indicating limited Fe oxide was formed on ZVI, because the reaction was conducted under anaerobic conditions. Overall, the strong correlation between the theoretical calculated Fe^{2+} concentrations and the actual detected Fe^{2+} concentrations (Figure 1e) and the formation of DCAcAm (Figure 1b) and MCAcAm (Figure 1c) suggest direct dechlorination of TCAcAm by ZVI was the primary operative reaction process, in agreement with the recent study discovering the direct reduction of Se (IV) by detecting Fe^{2+} release (Liang et al., 2014).

3.2. Integrated toxic risk caused by HAcAms during ZVI dehalogenation

Plewa and colleagues systematically investigated the cytotoxicity and genotoxicity of HAcAms (Plewa et al., 2008), and found the combined toxicity values (cytotoxicity plus genotoxicity) of MCAcAm (1310 M^{-1}) was significantly higher than DCAcAm (168 M^{-1}) and TCAcAm (233 M^{-1}) (Table SM2). To further compare the toxic effect of HAcAms during ZVI reductive dehalogenation,

we undertook a preliminary toxic risk analysis by calculating the toxic risk value of each HAcAm (Yang et al., 2013), obtained by multiplying the combined toxicity value (Plewa et al., 2008) by its concentration as recorded under different conditions during this study. Then, the integrated toxic risk value was calculated by summing values for the three chlorinated HAcAm (Table SM2), as shown in Figure 1f. The relative calculation formula is shown below:

$$ITRV_t = \Sigma [CTV_{HAcAm} \times C_{HAcAm,t}] \quad (8)$$

$ITRV_t$ — Integrated toxic risk value at t h

CTV_{HAcAm} — Combined toxicity value (M^{-1}) of each detected HAcAm

$C_{HAcAm,t}$ — Concentration of each HAcAm (nM) at t h

As shown in Figure 1f, at ZVI = 0.2 g/L, the integrated toxic risk value for the three chlorinated HAcAms over 24 h was stable due to low removal of TCAcAm. When the ZVI dosage was increased to 5.0 g/L, the integrated toxic risk decreased from the initial value of 1.20×10^6 to 5.76×10^5 at 6 h, and then increased to 9.02×10^5 at 12 h and 7.75×10^5 at 24h. This is mainly attributable to the formation of MCAcAm over long time periods (Figure 1c), as this compound has higher combined toxicity than DCAcAm and TCAcAm (Plewa et al., 2008, Table SM2). When the ZVI dose was further increased to 10.0 g/L, the pattern of integrated toxic risk values was similar to ZVI = 5.0 g/L, except that values were further decreased to 3.43×10^5 at 24 h due to removal of MCAcAm at the highest ZVI dose (10.0 g/L). Since MCAcAm, which has high combined toxicity, was not effectively removed, the ability of ZVI to dehalogenate HAcAms needs to be enhanced.

3.3. Removal of HAcAms by metallic Cu

As shown in Figure SM3, the concentrations of TCAcAm did not change significantly at applied Cu doses, and DCAcAm and MCAcAm were undetectable over 24 h. As DCAcAm and MCAcAm

were not formed from TCAcAm, the effect of Cu alone on reduction of DCAcAm and MCAcAm was investigated separately. The results showed that Cu alone was also not effective for the reduction of DCAcAm and MCAcAm. Therefore, it was confirmed that metallic Cu alone cannot effectively reduce the three chlorinated HAcAms in drinking water. This is because Cu(II) ($E^0_{[Cu2+/Cu]}$ = +0.34V at 25℃) has a significantly higher (more positive) reduction potential than Fe(II) ($E^0_{[Fe2+/Fe]}$ = -0.45V at 25℃) (Hoang et al., 2011).

3.4. Removal of HAcAms by ZVI/Cu

The impact of Cu addition on the reduction of HAcAms by ZVI was also investigated (Figure SM4). As seen, the dechlorination of TCAcAm was increased when Cu and ZVI were dosed together into TCAcAm solution. The pseudo-first-order reduction rate of TCAcAm increased from 0.43 h^{-1} (Table SM1) to 0.60 h^{-1} (Table SM3) when ZVI alone was changed to ZVI/Cu at ZVI/Cu molar ratio = 1:1 and pH = 7.0. Figure SM4 investigated the influence of ZVI/Cu molar ratio on the removal of HAcAms. The reduction in TCAcAm reached the optimal efficiency at a ZVI/Cu molar ratio of 1:1. 82.3% TCAcAm was reduced at ZVI dose = 10.0 g/L after 3 h. After 24 h, TCAcAm and DCAcAm were both undetectable at all selected ZVI/Cu molar ratios at ZVI dose = 10.0 g/L. Thus, only MCAcAm was detected and moreover MCAcAm was reduced to below the detection limit when the ZVI/Cu molar ratio was 1:1. In general, the addition of Cu strengthened the reductive dehalogenation of HAcAms by ZVI, and the optimal ZVI/Cu molar ratio was 1:1 for reduction of HAcAms. As previously reported, in the primary battery system, the potential difference between Fe and Cu (0.78 V) is even higher than that between Fe and Fe^{2+} (0.45 V), thereby the addition of Cu can accelerate corrosion of the ZVI surface and raise the reactivity of ZVI (Ma and Zhang, 2008;

285 Xiong et al., 2015). However, excess Cu can cover the reaction sites on the surface of ZVI, which
286 negatively impacts reduction (Jiao et al., 2009; Lai et al., 2014). Therefore, ZVI/Cu molar ratio of
287 1:1 was selected for subsequent tests.
288
289 **3.5. The impact of pH on the removal of chlorinated HAcAms by ZVI/Cu**
290
291 **[Figure 2]**
292
293 Figure 2 shows the effect of solution pH on the dechlorination of TCAcAm by ZVI and Cu at a
294 molar ratio of 1:1. As shown in Figure 2a, TCAcAm reduction rates (Table SM3) accelerated from
295 0.02 h^{-1} to 2.23 h^{-1} as pH decreased from 8.0 to 5.0, this result being similar to the previous reports
296 (Fang et al., 2011; Xia et al., 2014; Zhang et al, 2006; Jovanovic et al, 2005). At a relatively high
297 pH (e.g., pH = 8.0), a passivation layer (a layer formed by the corrosion products, such as $Fe(OH)_2$,
298 $Fe(OH)_3$, $FeCO_3$ and so on) can be produced on the surface of ZVI, which can suppress additional
299 dechlorination reaction of TCAcAm (Fang et al., 2011; Xia et al., 2014). However, since neither
300 DCAcAm (Figure 2b) nor MCAcAm (Figure 2c) was detected, this indicated the reduction of
301 TCAcAm was attributable to the base-catalyzed hydrolysis of HAcAms (Glezer et al., 1999; Chu et
302 al., 2009a). A previous study reported the hydrolysis rate constant of TCAcAm at pH = 8.0 was
303 0.015 h^{-1} (Chu et al., 2009a), which was slightly lower than the reduction rate constant (0.020 h^{-1},
304 Table SM3) recorded for TCAcAm at pH = 8.0 in the present study. When the reduction rate constant
305 (0.020 h^{-1}) was separated from the hydrolysis rate constant (0.015 h^{-1}), the remained reduction rate
306 constant (0.005 h^{-1}) was probably attributed to that a small amount of TCAcAm was probably
307 dechlorinated by ZVI/Cu at pH = 8.0, the DCAcAm formed could be hydrolyzed to DCAA (Glezer

et al., 1999; Chu et al., 2009a; Yu and Reckhow, 2015). To confirm this hypothesis, we analyzed the concentrations of three HAAs. At pH = 8.0, as shown in Figure 2e, the three HAAs were not detected during the initial 1 h, whereas TCAA concentrations at 3, 6, 12 and 24 h were 0.35 ± 0.02, 0.46 ± 0.02, 0.54 ± 0.03 and 0.77 ± 0.04 μM, respectively (Figure 2e). DCAA (0.14±0.01 μM) was also detected at 24 h, which is in agreement with the above-mentioned hypothesis and corresponds with results from previous studies examining the hydrolysis of haloacetonitriles and HAcAms (Chu et al., 2009a; Yu and Reckhow, 2015). MCAA was not detected, indicating dechlorination of neither of TCAcAm nor TCAA was significant under these conditions. This is consistent with a previous study which also found that ZVI/Cu may effectively remove HAAs in water at pH 7.0, but was ineffective under alkaline conditions (Chu et al., 2009b).

At lower pH values (e.g., pH = 5.0 and 6.0), all three HAAs were undetected (Figure 2e). This can be explained by limited hydrolysis of HAcAms to HAAs under acidic conditions (Chu et al., 2013; Yu and Reckhow, 2015). However, the ZVI corrosion (the reduction of ZVI to Fe^{2+}) was accelerated in a weakly acid environment, which can promote dechlorination of TCAcAm by Equation (2) (Noubactep, 2008; Zhang et al, 2006; Jovanovic et al, 2005). At pH 5.0 and pH 6.0, the concentrations of DCAcAm initially increased to 1.31 ± 0.07 μM and 1.49 ± 0.07 μM respectively at 1h, and then rapidly decreased to below the detection limit at 3 h (Figure 2b). Unlike DCAcAm, the concentrations of MCAcAm initially increased to 3.57 ± 0.18 μM and 2.17 ± 0.11 μM after 3 h at pH 5.0 and pH 6.0, respectively, and then slowly decreased to 2.44 ± 0.12 μM and 1.14 ± 0.06 μM at 24 h, respectively (Figure 2c). Of note, the reduction of MCAcAm at pH 5.0 and pH 6.0 was less than at pH 7.0, which also resulted in poorer removal for the sum of three HAcAms at pH 5.0 and pH 6.0 than pH 7.0 at 24 h (Figure 2d). As discussed in Section 3.1, limited Fe oxide

was formed on ZVI at pH 7.0, which potentially adsorbed a fraction of the MCAcAm formed.

As shown in Figure 2f, we also compared the integrated toxic risk values of HAcAms at different pHs (Table SM4). Although TCAcAm and DCAcAm were removed effectively at pH 5.0 and pH 6.0, the integrated toxic risk values (3.79×10^6 and 2.26×10^6 at 12 h) for the HAcAms were relatively higher than at pH = 7.0 (1.13×10^6 at 12 h), due to the poor removal of MCAcAm. Additionally, integrated toxic risk values for HAcAms at pH = 8.0 (9.76×10^5 at 12 h) were similar to at pH = 7.0 (1.13×10^6 at 12 h) before 12 h, mainly because MCAcAm with higher combined toxicity was not formed from the dechlorination of TCAcAm by ZVI/Cu at pH = 8.0. In general, the neutral condition was most conducive to the total removal of TCAcAm, DCAcAm and MCAcAm by ZVI/Cu.

3.6. The impact of temperature on the removal of HAcAms by ZVI/Cu

[Figure 3]

As shown in Figure 3, reduction of TCAcAm increased as the temperature increased from 10 °C to 40 °C. We calculated the activation energies (E_a) for the reaction between ZVI/Cu and TCAcAm using the Arrhenius plot (Arrhenius, 1889) and the pseudo first order reaction rate constants at different temperatures (Figure SM5). The E_a in the reaction between ZVI/Cu and TCAcAm is 52.8 kJ/mol. This is lower than that for many common chemical reactions (60~250 kJ/mol) (Laidler, 1993), which indicates the reaction is expected to proceed under ambient conditions. At 40 °C, TCAcAm was removed completely inside 3 h. DCAcAm and MCAcAm were both detected at 1 h, but were also both reduced to below the detection limits inside 3 h (see Figure SM6).. At 10 °C, the

352 reduction rates of three HAcAms were relatively slower than at 25 °C. The concentrations of
353 DCAcAm initially increased to 1.44 ±0.07 μM at 3 h, and then rapidly decreased to 0.98 ±0.05 μM
354 at 24 h. Further, concentrations of MCAcAm continuously increased over 24 h (from 0.30 ±0.02
355 μM at 3 h to 1.14 ±0.06 μM at 24 h). This also resulted in high integrated toxic risk value (1.71×10^6)
356 from the HAcAms at 24 h and 10 °C (Figure SM7 and Table SM5).
357
358 **3.7. Removal of brominated HAcAms by ZVI/Cu**
359 **[Figure 4]**
360
361 The dehalogenation of BDCAcAm, DBCAcAm and TBAcAm by ZVI/Cu was investigated at pH
362 6.0 ±0.2 to avoid the effect of hydrolysis of HAcAms (Chu et al., 2009a, 2013; Yu and Reckhow,
363 2015). The removal of three brominated HAcAms by ZVI at pH 6.0 was also investigated, and the
364 removal and formation trend of HAcAms was in agreement with that by ZVI/Cu. However, the
365 removal efficiency of HAcAm by ZVI was significantly inferior to ZVI/Cu (Figure SM8). As shown
366 in Figure 4a and 4b, DCAcAm and BCAcAm were firstly formed from the debromination of
367 BDCAcAm and BDCAcAm, respectively. Subsequently, DCAcAm and BCAcAm concentrations
368 was further decreased, and only MCAcAm was recorded from the dechlorination and debromination
369 of DCAcAm and BCAcAm, respectively. This results directly suggests that bromine was
370 preferentially removed over chlorine in HAcAms by ZVI/Cu.
371 Because of this, BDCAcAm, DBCAcAm and TBAcAm concentrations were all rapidly
372 reduced to a very low levels (near the detection limit) inside 1 h (Figure 4a, 4b and 4c), and the
373 removal rates (98.7%, 97.6% and 96.4%) of three brominated HAcAms were all higher than for

TCAcAm (84.3%) under the same reaction conditions (Figure SM9). Additionally, as shown in Figure 4c, only MBAcAm was observed from 3 h to 24 h, and only MCAcAm was left from 3 h to 24 h for BDCAcAm (Figure 4a), DBCAcAm (Figure 4b) and TCAcAm (Figure 4d) at pH 6.0. Therefore, a plot of the pseudo-first-order reduction rate of MCAcAm (from dehalogenation of TCAcAm, BDCAcAm and DBCAcAm) and MBAcAm (from TBAcAm) from 3 h to 24 h is presented in Figure 4e. The reduction rate for MBAcAm (k_{obs} = 0.079 h^{-1}) was comparatively higher than for MCAcAm (k_{obs} = 0.030, 0.036 and 0.037 h^{-1}). These results all indicated that brominated HAcAms were more easily reduced than chlorinated HAcAms by ZVI/Cu, which is in agreement with a previous study examining the removal of HAAs by ZVI (Hozalski et al., 2001). Although the electronegativity of chloride (3.16) is greater than bromine (2.96), the bond length of the C-Br bond (194×10^{-12} m) is higher than the C-Cl bond (177×10^{-12} m) (Haynes, 2013; Linus, 1932), which equates to the former being weaker than the latter (March, 1992).

Figure 4f compares the integrated toxic risk from TCAcAm, BDCAcAm, DBCAcAm, and TBAcAm during ZVI/Cu reduction. After 3 h, the integrated toxic risk from reduced solutions of TCAcAm, BDCAcAm and DBCAcAm all decreased, whereas the integrated toxic risk from TBAcAm was higher from 3 h (6.58×10^7) to 24 h (1.23×10^7), because only TBAcAm, which has high combined toxicity (Table SM6), formed MBAcAm during ZVI/Cu dehalogenation reduction under these conditions. Therefore, reduction of TBAcAm caused a higher toxicity risk than reductions of TCAcAm, even though TBAcAm was more easily dehalogenated than TCAcAm by ZVI/Cu dehalogenation.

4. Conclusions

ZVI alone can dechlorinate TCAcAm to sequentially form DCAcAm and MCAcAm. The strong correlation between the theoretical calculated Fe^{2+} concentrations and the actual detected Fe^{2+} concentrations release suggests the reduction of TCAcAm is mainly attributable to direct dechlorination of TCAcAm by ZVI. At increased ZVI doses, the reduction rate of TCAcAm was accelerated, and the integrated toxic risks caused by total concentrations of TCAcAm, DCAcAm and MCAcAm decreased.

Metallic Cu alone did not affect HAcAm concentrations, but the addition of Cu to ZVI significantly improved the removal of HAcAms during ZVI dehalogenation. TCAcAm and its reduction products (DCAcAm and MCAcAm) were all decreased to under detection limits at a ZVI/Cu molar ratio of 1:1 and 24 h.

Dechlorination of TCAcAm by ZVI/Cu increased with the decreasing pH from 8.0 to 5.0. The slight decrease in TCAcAm concentration at pH = 8.0 was explained by base-catalyzed hydrolysis of HAcAms, rather than dechlorination of TCAcAm by ZVI/Cu. Under acidic conditions TCAcAm dechlorination reaction was promoted, while the integrated toxic risk was minimised at pH 7.0, due to poor removal of the reduction product MCAcAm at pH = 5.0 and 6.0. Additionally, the reductive dehalogenation of HAcAms had a low E_a value, and was increased at the temperature increased from 10 ^oC to 25 ^oC to 40 ^oC. The lower temperature resulted in higher integrated toxic risk value due to the increased formation of MCAcAm.

Bromine was preferentially removed over chlorine in HAcAms during ZVI/Cu dehalogenation, as higher overall removal of brominated HAcAms than chlorinated HAcAms was recorded. However, TBAcAm caused higher integrated toxicity risk than TCAcAm, even though TBAcAm

was more easily removed than TCAcAm during ZVI/Cu reduction, due to the formation of MBAcAm during debromination of TBAcAm.

In distribution systems, any ZVI present in the passive layer of cast iron pipes will come into contact with treated water. This highlights the potential for the formation of monohaloacetamides (MCAcAm and MBAcAm), with higher toxicity than trihaloacetamides and dihaloacetamides, from ZVI-mediated reactions during drinking water distribution. This study demonstrates that higher ZVI/Cu exposure - 10 g/L ZVI and 11 g/L Cu - effectively reduces the integrated toxicity risks (based on combined cytotoxicity and genotoxicity) at neutral conditions and ambient temperatures. However, investigations at pilot- and/or full-scale are required to fully understand the magnitude of reductive dehalogenation which occurs in real-life distribution systems.

Acknowledgements

The authors gratefully acknowledge the National Natural Science Foundation of China (No. 51378366, 51578389), and the National Major Science and Technology Project of China (No. 2015ZX07406004).

Appendix A. Supplementary data

Supplementary data related to this article is available in this appendix.

REFERENCES

Arrhenius, S.A., 1889. Über die Dissociationswärme und den Einfluß der Temperatur auf den Dissociationsgrad der Elektrolyte. Z. Phys. Chem. 4, 96-116.

Bond, T., Huang, J., Templeton, M.R., Graham, N., 2011. Occurrence and control of nitrogenous disinfection by-products in drinking water - A review. Water Res. 45 (15), 4341-4354.

Bond, T., Templeton, M.R., Mokhtar K., Nurul H., Graham, N., Kanda, R., 2015. Nitrogenous disinfection byproducts in English drinking water supply systems: occurrence, bromine substitution and correlation analysis. Water Res. 85, 85-94.

Chu, W.H., Gao, N.Y., Deng, Y., 2009a. Stability of new found nitrogenous disinfection by-products: haloacetamides in drinking water. Chin. J. Org. Chem. 29 (10), 1569-1574.

Chu, W.H., Gao, N.Y., Zhao, S.J., Dong, B.Z., 2009b. Removal of halogenated disinfection by-products trichloroacetic acid by Fe/Cu catalytic reduction in drinking water. Journal of Tongji University (Natural Science) 37 (10), 1355-1359.

Chu, W.H., Gao, N.Y., Deng, Y., Templeton, M.R., Yin, D.Q., 2011. Impacts of drinking water pretreatments on the formation of nitrogenous disinfection by-products. Bioresource Technol. 102 (24), 11161-11166.

Chu, W.H., Gao, N.Y., Yin, D.Q., Krasner, S.W., Templeton, M.R., 2012. Trace determination of 13 haloacetamides in drinking water using liquid chromatography triple quadrupole mass spectrometry with atmospheric pressure chemical ionization. J. Chromatogr. A. 1235, 178-181.

Chu, W.H., Gao, N.Y., Yin D.Q., Krasnerb, S.W., 2013. Formation and speciation of nine haloacetamides, an emerging class of nitrogenous DBPs, during chlorination or chloramination. J. Hazard. Mater. 260, 806-812.

Chu, W.H., Gao, N.Y., Yin, D.Q., et al., 2014. Impact of UV/H_2O_2 pre-oxidation on the formation of haloacetamides and other nitrogenous disinfection byproducts during chlorination. Environ. Sci. Technol. 48 (20), 12190-12198.

Chu, W.H., Li, D.M., Gao, N.Y., et al., 2015a. The control of emerging haloacetamide DBP

precursors with UV/persulfate treatment. Water Res. 72, 340-348.

Chu, W.H., Li, X., Gao, N.Y., et al, 2015b. Peptide bonds affect the formation of haloacetamides, an emerging class of N-DBPs in drinking water: free amino acids versus oligopeptides.Sci. Rep. 5, 14412.

Critchley, M.M., Cromar, N.J., McClure, N., Fallowfield, H.J., 2001. Biofilms and microbially influenced cuprosolvency in domestic copper plumbing systems. J. Appl. Microbiol., 91, 646-651.

Cwiertny, D.M., Bransfield, S.J., Livi, K.J.T., Fairbrother, D.H., Roberts, A.L., 2006. Exploring the influence of granular iron additives on 1,1,1-trichloroethane reduction. Environ. Sci. Technol. 40 (21), 6837-6843.

Dotson, A., Westerhoff, P., 2009. Occurrence and removal of amino acids during drinking water treatment. J. Am. Water Work Assoc. 101 (9), 101-115.Dries, J., Bastiaens, L., Springael, D., Agathos, S.N., Diels, L., 2004. Competition for sorption and degradation of chlorinated ethenes in batch zero-valent iron systems. Environ. Sci. Technol. 38 (10), 2879-2884.

Fang, Z.Q., Chen, J.H., Qiu, X.H., Qiu, X.Q., Cheng, W., Zhu, L.C., 2011. Effective removal of antibiotic metronidazole from water by nanoscale zero-valent iron particles. Desalination 268, 60-67.

Feng, J., Lim, T.T., 2007. Iron-mediated reduction rates and pathways of halogenated methanes with nanoscale Pd/Fe: analysis of linear free energy relationship. Chemosphere 66 (9), 1765-1774.

Gillham, R.W., O'Hannesin, S.F., 1994. Enhanced degradation of halogenated aliphatics by zero-valent iron. Ground Water 32 (6), 958-967.

Glezer, V., Harris, B., Tal, N., Iosefzon, B., Lev, O., 1999. Hydrolysis of haloacetonitriles: linear free energy relationship, kinetics and products. Water Res. 33, 1938-1948.

Goslan, E.H., Krasner, S.W., Bower, M., Rocks, S.A., Holmes, P., Levy, L.S., Parsons, S.A., 2009. A comparison of disinfection by-products found in chlorinated and chloraminated drinking waters in Scotland. Water Res. 43 (18), 4698-4706.

Guan, X.H., Sun, Y.K., Qin, H.J., Li, J.X., Lo, I.M.C., He, D., Dong, H.R., 2015. The limitations of applying zero-valent iron technology in contaminants sequestration and the corresponding countermeasures: the development in zero-valent iron technology in the last two decades (1994-2014). Water Res. 75, 224-248.

Guo, X.J., Yang, Z., Liu, H., Lv, X.F., Tu, Q.S., Ren, Q.D., Xia, X.H., Jing, C.Y., 2015. Common oxidants activate the reactivity of zero-valent iron (ZVI) and hence remarkably enhance nitrate reduction from water. Sep. Purif. Technol. 146, 227-234.

He, F., Zhao, D.Y., Paul, C., 2010. Field assessment of carboxymethyl cellulose stabilized iron nanoparticles for in situ destruction of chlorinated solvents in source zones. Water Res. 44, 2360-2370.

Haynes, W.M., 2013. CRC Handbook of Chemistry and Physics, 94th ed. CRC Press, Boca Raton, FL

Hoang, D.L., Dang, T.T.H., Engeldinger, J., Schneider, M., Radnik, J., Richter, M., Martin, A., 2011. TPR investigations on the reducibility of Cu supported on Al_2O_3, zeolite Y and SAPO-5. J. Solid State Chem. 184, 1915-1923.

Hou, Y.K., Chu, W.H., Ma, M., 2012. Carbonaceous and nitrogenous disinfection by-product formation in the surface and ground water treatment plants using Yellow River as water

source. J. Environ. Sci. 24 (7), 1204-1209.

House, H.O., 1972. Modern synthetic reactions. Second ed, Benjamin, Menlo Park, CA, 145-227.

Hozalski, R.M., Li, Z., Arnold, W.A., 2001. Reduction of haloacetic acids by Fe0: implications for treatment and fate. Environ. Sci. Technol. 35, 2258-2263.

Huang, H., Wu, Q.Y., Hu, H.Y., Mitch, W.A., 2012. Dichloroacetonitrile and dichloroacetamide can form independently during chlorination and chloramination of drinking waters, model organic matters, and wastewater effluents. Environ. Sci. Technol. 46 (19), 10624-10631.

Jiao, Y.L., Qiu, C.C., Huang, L.H., Wu, K.X., Ma, H.Y., Chen, S.H., Ma, L.M., Wu, D.L., 2009. Reductive dechlorination of carbon tetrachloride by zero-valent iron and related iron corrosion. Appl. Catal. B-Environ. 91 (1-2), 434-440.

Jovanovic, G.N., Znidarsic-Plazl, P., Sakrittichai, P., Al-Khaldi, K., 2005. Dechlorination of p-chlorophenol in a microreactor with bimetallic Pd/Fe catalyst, Ind. Eng. Chem. Res. 44, 5099-5106.

Keenan, C.R., Sedlak, D.L., 2008. Factors affecting the yield of oxidants from the reaction of manoparticulate zero-valent iron and oxygen. Environ. Sci. Technol. 42 (4), 1262-1267.

Kohn, T., Livi, K.J.T., Roberts, A.L., Vikesland, P.J., 2005. Longevity of granular iron in groundwater treatment processes: corrosion product development. Environ. Sci. Technol. 39 (8), 2867-2879.

Kooij, D.v.d., Veenendaal, H.R., Scheffer, W.J.H., 2005. Biofilm formation and multiplication of *Legionella* in a model warm water system with pipes of copper, stainless steel and cross-linked polyethylene. Water Res. 39 (13), 2789-2798.

Krasner, S.W., Mitch, W.A, McCurry, D.L., Hanigan, D., Westerhoff, P., 2013. Formation,

precursors, control, and occurrence of nitrosamines in drinking water: a review. Water Res. 47 (13), 4433-4450.

Krasner, S.W., Weinberg, H.S., Richardson, S.D., Pastor, S.J., Chinn, R., Sclimenti, M.J., Onstad, G.D., Thruston, A.D., 2006. Occurrence of a new generation of disinfection byproducts. Environ. Sci. Technol. 40 (23), 7175-7185.

Lai B., Zhang, Y.H., Chen, Z.Y., Yang, P., Zhou, Y.X., Wang, J.L., 2014. Removal of ρ-nitrophenol (PNP) in aqueous solution by the micro-scale iron-copper (Fe/Cu) bimetallic particles. Appl. Catal. B-Environ. 144, 816-830.

Laidler, K. J. 1993. The World of Physical Chemistry. Oxford University Press, Oxford.

Lehtola, M.J., Miettinen, I.T., Keinänen, M.M., Kekki, T.K., Laine, O., Hirvonen, A., Vartiainen, T., Martikainen, P.J., 2004. Microbiology, chemistry and biofilm development in a pilot drinking water distribution system with copper and plastic pipes. Water Res. 38 (17), 3769-3779.

Liang, L.P., Guan, X.H., Shi, Z., Li, J.L., Wu, Y.N., Paul, G.T., 2014. Coupled effects of aging and weak magnetic fields on sequestration of selenite by zero-valent iron. Environ. Sci. Technol. 48 (11), 6326-6334.

Lien, H.L., Zhang, W.X., 2001. Nanoscale iron particles for complete reduction of chlorinated ethenes. Colloids Surf., A: Physicochemical and Engineering Aspects 191 (1-2), 97-105.

Lien, H.L., Zhang, W.X., 2005. Hydrodechlorination of chlorinated ethanes by nanoscale Pd/Fe bimetallic particles. J. Environ. Eng. 131 (1), 4-10.

Lin, J.P., Ellaway, M., Adrien, R., 2001. Study of corrosion material accumulated on the inner wall of steel water pipe. Corros. Sci. 43 (11), 2065-2081.

550 Linus, P., 1932. The nature of the chemical bond. iv. The energy of single bonds and the relative
551 electronegativity of atoms. J. Am. Chem. Soc. 54 (9), 3570-3582.
552 Liu, Y.Q., Lowry, G.V., 2006. Effect of particle age (Fe^0 content) and solution pH on NZVI
553 reactivity: H_2 evolution and TCE dechlorination. Environ. Sci. Technol. 40 (19), 6085-
554 6090.
555 Liu, J., Zhang, X.R., 2014. Comparative toxicity of new halophenolic DBPs in chlorinated saline
556 wastewater effluents against a marine alga: Halophenolic DBPs are generally more toxic
557 than haloaliphatic ones. Water Res. 65, 64-72.
558 Liu, X., Zhang, Y., Han, W., Tang, A., Shen, J., Cui, Z., Vitousek, P., Erisman, J.W., Goulding, K.,
559 Christie, P., Fangmeier, A., Zhang, F., 2013. Enhanced nitrogen deposition over china.
560 Nature 494 (7438), 459-462.
561 Ma, L.M., Zhang, W.X., 2008. Enhanced biological treatment of industrial wastewater with
562 bimetallic zero-valent iron. Environ. Sci. Technol. 42 (15), 5384-5389.
563 Magazinovic, R.S., Nicholson, B.C., Mulcahy, D.E., Davey, D.E., 2004. Bromide levels in natural
564 waters: its relationship to levels of both chloride and total dissolved solids and the
565 implications for water treatment. Chemosphere 57 (4), 329-335.
566 March, J., 1992. Advanced organic chemistry, Wiley-Interscience: New York.
567 McNeill, L.S., Edwards, M., 2001. Iron pipe corrosion in distribution systems. J. Am. Water Works
568 Ass. 93 (7), 88-101.
569 Niquette, P., Servais, P., Savoir, R., 2000. Impacts of pipe materials on densities of fixed bacterial
570 biomass in a drinking water distribution system. Water Res. 34 (6), 1952-1956.
571 Noubactep, C., 2008. A critical review on the process of contaminant removal in Fe^0-H_2O systems.

572 Environ. Sci. Technol. 29 (8), 909-920.
573 Plewa, M.J., Muellner, M.G., Richardson, S.D., Fasano, F., Buettner, K.M., Woo, Y.T., McKague,
574 A.B., Wagner, E.D., 2008. Occurrence, synthesis, and mammalian cell cytotoxicity and
575 genotoxicity of haloacetamides: an emerging class of nitrogenous drinking water
576 disinfection byproducts. Environ. Sci. Technol. 42 (3), 955-961.
577 Plewa, M.J., and Wanger, E.D., 2015. Charting a new path to resolve the adverse health effects of
578 DBPs, In Recent Advances in Disinfection By-Products; Karanfil, Karanfil, Tanju, Bill
579 Mitch, Paul Westerhoff, Yuefeng Xie; Chapter 1, 3-23. American Chemical Society:
580 Washington, DC.
581 Plewa, M.J., Wagner, E.D., Muellner, M.G., Hsu, K.M., Richardson, S.D., 2007. Comparative
582 mammalian cell toxicity of N-DBPs and C-DBPs, In ACS symposium series. Oxford
583 University Press, 2007.
584 Reckhow, D.A., Platt, T.L., MacNeill, A.L., McClellan, J.N., 2001. Formation and degradation of
585 dichloroacetonitrile in drinking waters. J. Water Supply Res. Technol. - Aqua. 50 (1), 1-13.
586 Richardson, S.D., Plewa, M.J., Wagner, E.D., Schoeny, R., DeMarini, D.M., 2007. Occurrence,
587 genotoxicity, and carcinogenicity of regulated and emerging disinfection by-products in
588 drinking water: a review and roadmap for research. Mutation. Res. 636 (1-3), 178-242.
589 Richardson, S.D., Postigo, C., 2015. Formation of DBPs: State of the Science, In Recent Advances
590 in Disinfection By-Products; Karanfil, Tanju, Bill Mitch, Paul Westerhoff, Yuefeng Xie;
591 Chapter 11, 189-214. American Chemical Society: Washington, DC.
592 Richardson, S.D., Ternes, T.A., 2014. Water analysis: emerging contaminants and current issues.
593 Anal. Chem. 86 (6), 2813-2848.

Richardson, S.D., Thruston Jr, A.D., Krasner, S.W., Weinberg, H.S., Miltner, R.J., Schenck, K.M., Narotsky, M.G., McKague, A.B., Simmons, J.E., 2008. Integrated disinfection by-products mixtures research: comprehensive characterization of water concentrates prepared from chlorinated and ozonated/postchlorinated drinking water. J. Toxicol. Environ. Health, Pt. A. 71 (17), 1165-1186.

Richardson, S.D., and Postigo, C., 2015. Formation of DBPs: State of the Science, In Recent Advances in Disinfection By-Products; Karanfil, Tanju, Bill Mitch, Paul Westerhoff, Yuefeng Xie; Chapter 11, 189-214. American Chemical Society: Washington, DC.

Ridgway, H.F., Means, E.G., Olson, B.H., 1981. Iron bacteria in drinking-water distribution systems: elemental analysis of *Gallionella* stalks, using X-ray energy-dispersive microanalysis. Appl. Environ. Microb. 41 (1), 288-297.

Rossman, L.A. Brown, R.A. Singer, P.C. Nuckols, J.R., 2001. DBP formation kinetics in a simulated distribution system, Water Res. 35(14), 3483-3489.

Shah, A.D., Krasner, S.W., Lee, C.F.T., von Gunten, U., Mitch, W.A., 2012. Trade-offs in disinfection byproduct formation associated with precursor preoxidation for control of N-Nitrosodimethylamine formation. Environ. Sci. Technol. 46 (9), 4809-4818.

Shah, A.D., Mitch, W.A., 2012. Halonitroalkanes, halonitriles, haloamides, and N-nitrosamines: a critical review of nitrogenous disinfection byproduct formation pathways. Environ. Sci. Technol. 46 (1), 119-131.

Tee, Y.H., Bachas, L., Bhattacharyya, D., 2009. Degradation of trichloroethylene by iron-based bimetallic nanoparticles. J. Phys. Chem. C 113 (28), 12616-12616.

Teng, F., Guan, Y.T., Zhu, W.P., 2008. Effect of biofilm on cast iron pipe corrosion in drinking water

distribution system: corrosion scales characterization and microbial community structure investigation. Corros. Sci. 50 (10), 2816-2823.

US EPA (1995) Method 552.2: determination of haloacetic acids and dalapon in drinking water by liquid–liquid extraction, derivatization and gas chromatography with electron capture detection. *Environmental Monitoring and System Laboratory, Cincinnati, OH.*

Wang, C.B., Zhang, W.X., 1997. Synthesizing nanoscale iron particles for rapid and complete dechlorination of TCE and PCBs, Environ. Sci. Technol. 31, 2154-2156.

Wang, X.Y., Chen, C., Chang, Y., Liu, H.L., 2009. Dechlorination of chlorinated methanes by Pd/Fe bimetallic nanoparticles. J. Hazard. Mater. 161 (2-3), 815-823.

Wang, Y., Le, R.J., Zhang, T., Croué, J.P., 2014. Formation of brominated disinfection byproducts from natural organic matter isolates and model compounds in a sulfate radical-based oxidation process. Environ. Sci. Technol. 48 (24), 14534-14542.

Warren, K.D., Arnold, R.G., Bishop, T.L., Lindholm, L.C., Betterton, E.A., 1995. Kinetics and mechanism of reductive dehalogenation of carbon tetrachloride using zero-valence metals. J. Hazard. Mater. 41 (2-3), 217-227.

Xia, S.Q., Gu, Z.L., Zhang, Z.Q., Zhang, J., Slawomir W.H., 2014. Removal of choramphenicol from aqueous solution by nanoscale zero-valent iron particles. Chem. Eng. J. 257, 98-104.

Xie, P.C., Ma, J., Fang, J.Y., Guan, Y.H., Yue, S.Y., Li, X.C., Chen, L.W., 2013. Comparison of permanganate preoxidation and preozonation on algae containing water: cell integrity, characteristics, and chlorinated disinfection byproduct formation. Environ. Sci. Technol. 47 (24), 14051-14061.

Xiong, Z., Lai, B., Yang, P., Zhou, Y., Wang, J., Fang, S., 2015. Comparative study on the reactivity

638 of Fe/Cu bimetallic particles and zero valent iron (ZVI) under different conditions of N_2,
639 air or without aeration. J. Hazard. Mater. 297, 261-268.
640 Yang, F., Zhang, J., Chu, W.H., Yin, D.Q., Templeton, M.R., 2014. Haloacetamides versus
641 halomethanes formation and toxicity in chloraminated drinking water. J. Hazard. Mater.
642 274, 156-163.
643 Yang, M.T., Zhang, X.R., 2013. Comparative developmental toxicity of new aromatic halogenated
644 DBPs in a chlorinated saline sewage effluent to the marine polychaete platynereis dumerilii.
645 Environ. Sci. Technol. 47 (19), 10868-10876.
646 Yu, Y., Reckhow, D.A., 2015. Kinetic analysis of haloacetonitrile stability in drinking waters.
647 Environ. Sci. Technol. 49 (18), 11028-11036.
648 Yu, S.L., Lin, T., Chen, W., Tao, H., 2015. The toxicity of a new disinfection by-product, 2,2-
649 dichloroacetamide (DCAcAm), on adult zebrafish (Danio rerio) and its occurrence in the
650 chlorinated drinking water. Chemosphere 139, 40-46.
651 Zhang, W.H., Quan, X., Wang, J.X., Zhang, Z.Y., Chen, S. 2006. Rapid and complete dechlorination
652 of PCP in aqueous solution using Ni-Fe nanoparticles under assistance of ultrasound,
653 Chemosphere 65, 58-64.
654 Zhang, W.X., Wang, C.B., Lien, H.L., 1998. Treatment of chlorinated organic contaminants with
655 nanoscale bimetallic particles. Catal. Today 40 (4), 387-395.
656 Zhang, X.L., Deng, B.L., Guo, J., Wang, Y., Lan, Y.Q., 2011. Ligand-assisted degradation of carbon
657 tetrachloride by microscale zero-valent iron. J. Environ. Manage. 92 (4), 1328-1333.
658 Zhang, Y., Zhang, Z.Y., Zhao, Y.P., Cheng, S.P., Ren, H.Q., 2013. Identifying health effects of
659 exposure to trichloroacetamide using transcriptomics and metabonomics in mice (Mus

musculus). Environ. Sci. Technol. 47 (6), 2918-2924.

Figure captions

Figure 1. Influence of ZVI dosage on the removal of HAcAms. (Initial TCAcAm molar concentration = 5.30 μM [DCAcAm and MCAcAm were not added]; **Figure 1a**, TCAcAm; **Figure 1b**, DCAcAm; **Figure 1c**, MCAcAm; **Figure 1d**, total HAcAms [sum of three HAcAm concentrations]; **Figure 1e**, comparison of the theoretical calculated Fe^{2+} concentrations and the actual detected Fe^{2+} concentrations; **Figure 1f**, integrated toxic risk caused by HAcAms at different ZVI dosages. The presented data in the Figure 1a, 1b, and 1c are averages of three observations. Their relative standard deviations (n = 3) are below 7%.

Figure 2. Influence of pH on the removal of HAcAms by ZVI/Cu. (Initial TCAcAm molar concentration = 5.30 μM [DCAcAm and MCAcAm were not added]. ZVI dosage = 10.0 g/L [ZVI/Cu molar ratio = 1:1]. The presented data in the Figure 1a, 1b, 1c and 1e are averages of three observations. Their relative standard deviations (n = 3) are below 10%.

Figure 3. Influence of temperature on the removal of HAcAms by ZVI/Cu. (Initial TCAcAm molar concentration = 5.30 μM [DCAcAm and MCAcAm were not added]. ZVI dosage = 10.0 g/L [ZVI/Cu molar ratio = 1:1]. The presented data in the Figure 1a, 1b and 1c are averages of three observations. Their relative standard deviations (n = 3) are below 7%.

Figure 4. Removal of brominated HAcAms by ZVI/Cu at pH 6.0. (Initial tri-brominated HAcAm molar concentration = 5.30 μM [BDCAcAm, DBCAcAm and TBAcAm were added for Figure 4a, 4b and 4c]; ZVI dosage = 10.0 g/L [ZVI/Cu molar ratio = 1:1]; **Figure 4a**, BDCAcAm removal; **Figure 4b**, DBCAcAm removal; **Figure 4c**, TBAcAm removal; **Figure 4d**, removal rate (%) of four tri-HAcAms at 1 h by ZVI/Cu; **Figure 4e**, the pseudo-first-order reduction rate of MCAcAm [Figure 4a and 4b] and MBAcAm [Figure 4c] from 3 h to 24 h; **Figure 4f**, integrated toxic risk caused by HAcAms at pH 6.0. The presented data in the Figure 1a, 1b and 1c are averages of three observations. Their relative standard deviations (n = 3) are below 7%.

692 **Revised Figure 1**

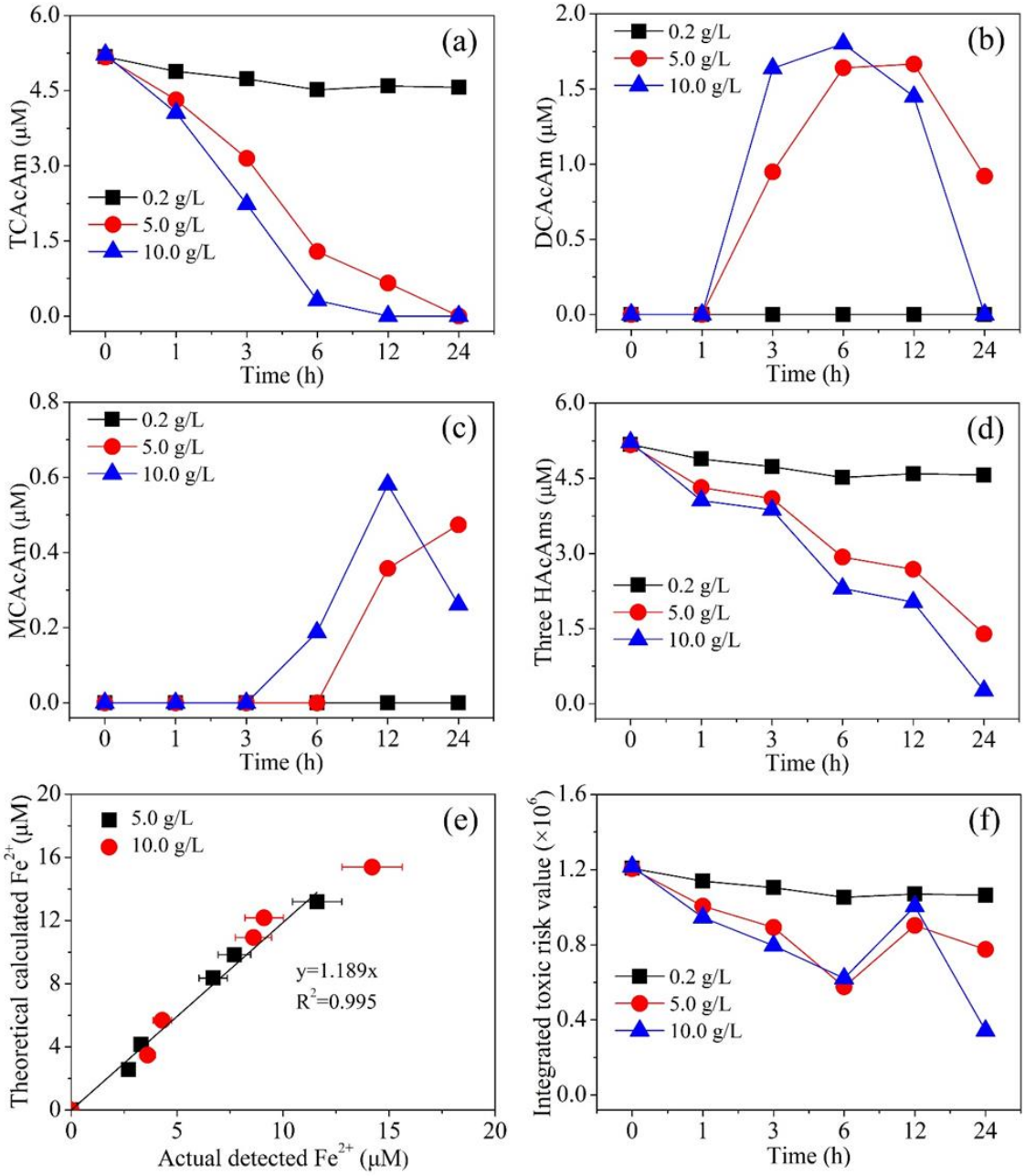

693

694 **Figure 1. Influence of ZVI dosage on the removal of HAcAms.** (Initial TCAcAm molar
695 concentration = 5.30 μM [DCAcAm and MCAcAm were not added]; **Figure 1a**, TCAcAm; **Figure**
696 **1b**, DCAcAm; **Figure 1c**, MCAcAm; **Figure 1d**, total HAcAms [sum of three HAcAm
697 concentrations]; **Figure 1e**, comparison of the theoretical calculated Fe^{2+} concentrations and the
698 actual detected Fe^{2+} concentrations; **Figure 1f**, integrated toxic risk caused by HAcAms at different
699 ZVI dosages.)

700

Revised Figure 2

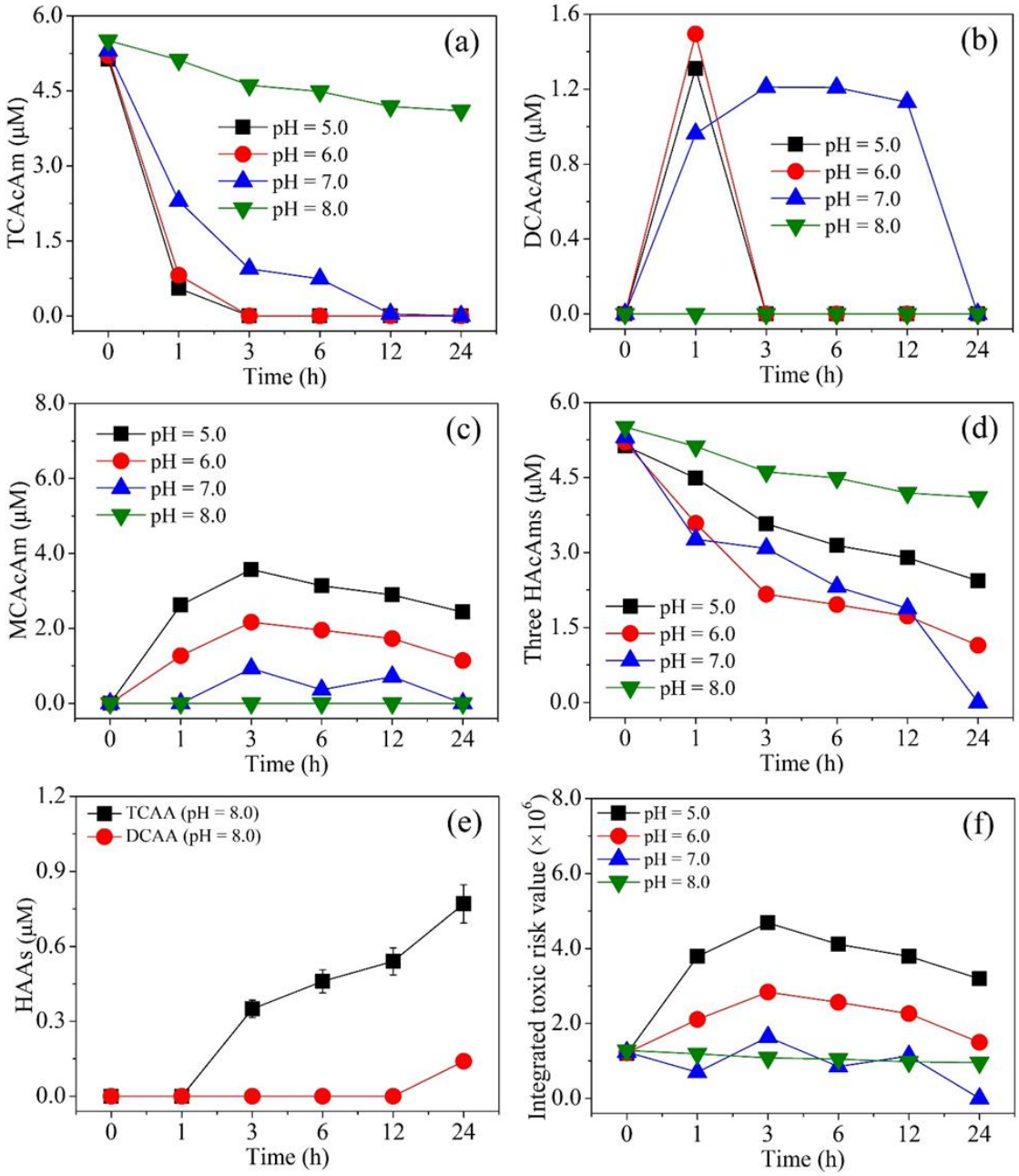

Figure 2. Influence of pH on the removal of HAcAms by ZVI/Cu. (Initial TCAcAm molar concentration = 5.30 μM [DCAcAm and MCAcAm were not added]. ZVI dosage = 10.0 g/L [ZVI/Cu molar ratio = 1:1])

Figure 3

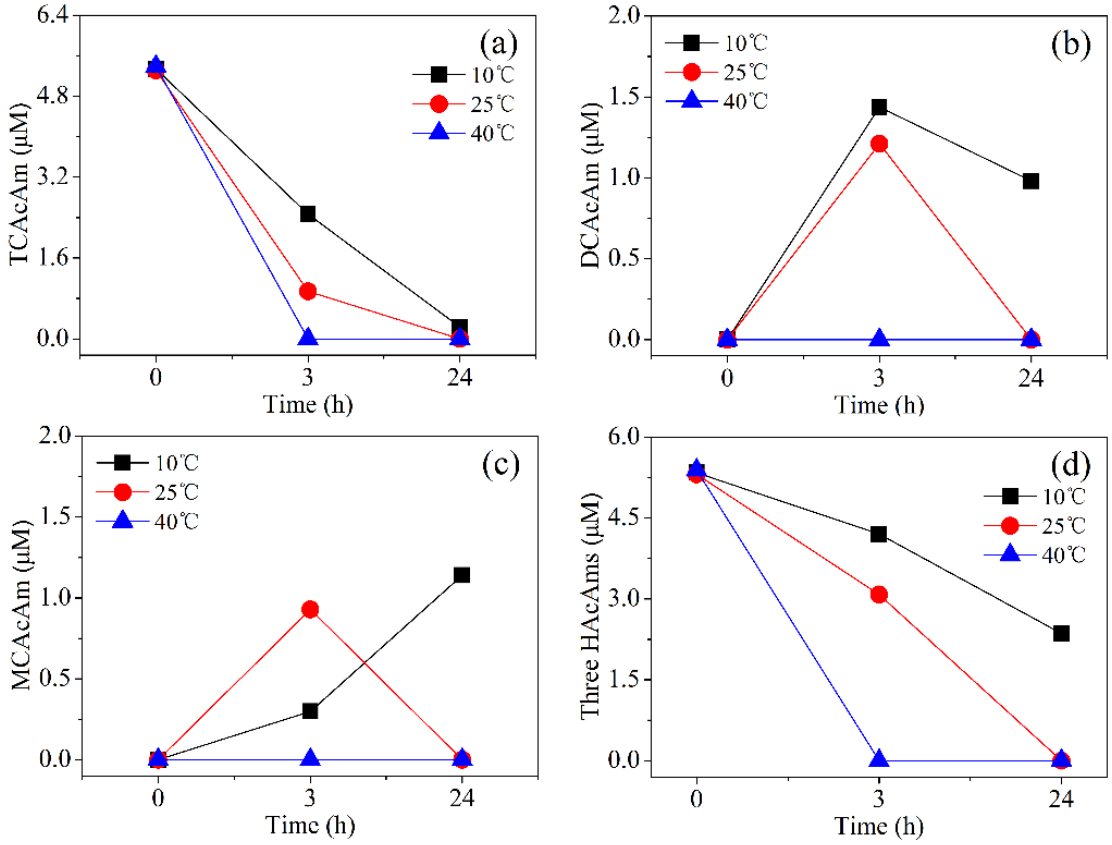

Figure 3. Influence of temperature on the removal of HAcAms by ZVI/Cu. (Initial TCAcAm molar concentration = 5.30 μM [DCAcAm and MCAcAm were not added]. ZVI dosage = 10.0 g/L [ZVI/Cu molar ratio = 1:1])

Figure 4

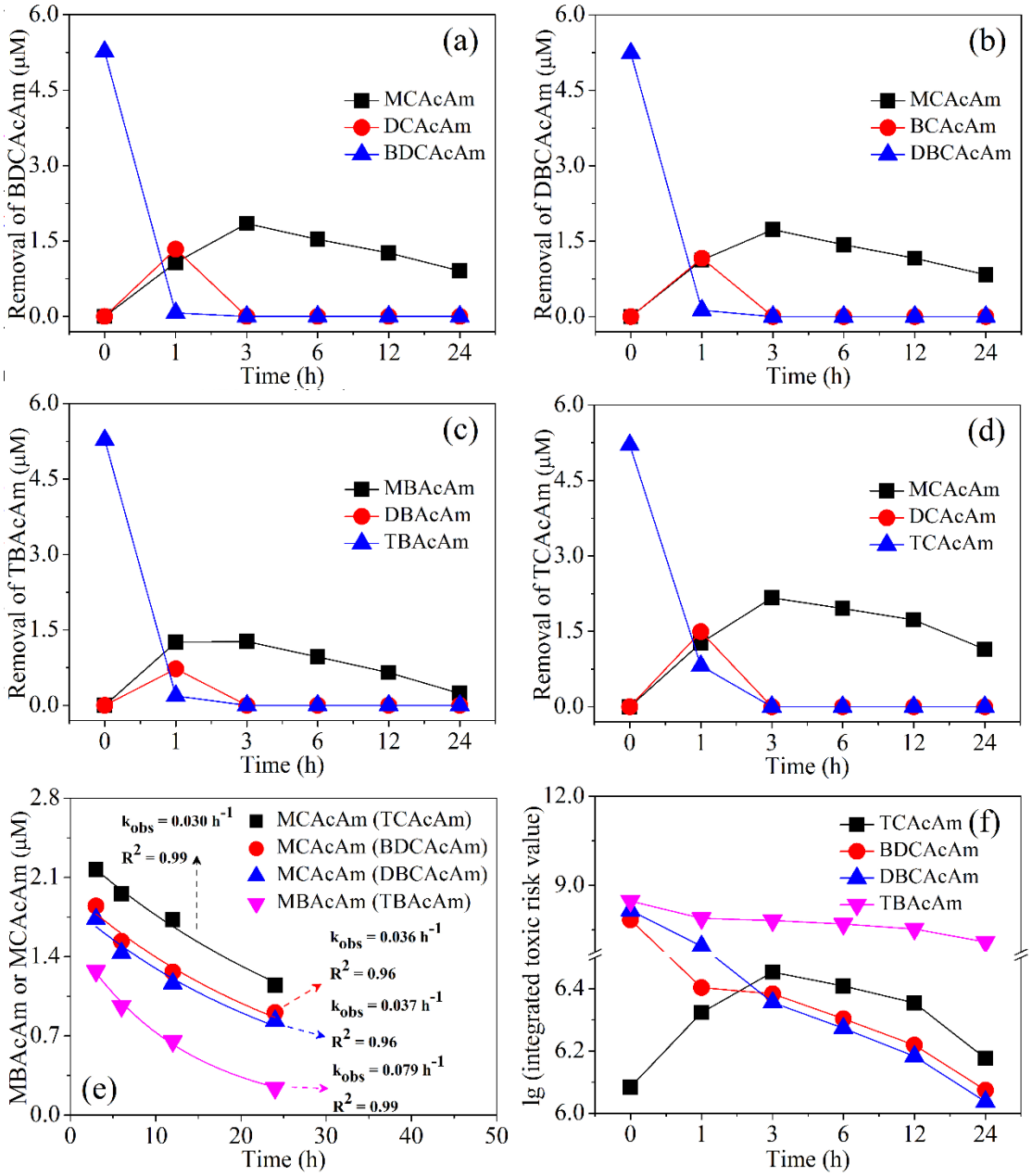

Figure 4. Removal of brominated HAcAms by ZVI/Cu at pH 6.0. (Initial tri-brominated HAcAm molar concentration = 5.30 μM [BDCAcAm, DBCAcAm and TBAcAm were added for Figure 4a, 4b and 4c]; ZVI dosage = 10.0 g/L [ZVI/Cu molar ratio = 1:1]; **Figure 4a**, BDCAcAm removal; **Figure 4b**, DBCAcAm removal; **Figure 4c**, TBAcAm removal; **Figure 4d**, removal rate (%) of four tri-HAcAms at 1 h by ZVI/Cu; **Figure 4e**, the pseudo-first-order reduction rate of MCAcAm [Figure 4a and 4b] and MBAcAm [Figure 4c] from 3 h to 24 h; **Figure 4f**, integrated toxic risk caused by HAcAms at pH 6.0.)